Plasmid DNA Cleavage by *Mun*I Restriction Enzyme: Single-Turnover and Steady-State Kinetic Analysis†

Giedrius Sasnauskas,‡ Albert Jeltsch,§ Alfred Pingoud,§ and Virginijus Siksnys*,‡

Institute of Biotechnology, Graiciuno 8, Vilnius 2028, Lithuania, and Institut fuer Biochemie Fachbereich Biologie, Justus-Liebig-Universitaet, Heinrich-Buff-Ring 58, D-35392 Giessen, Germany

Received October 14, 1998; Revised Manuscript Received January 21, 1999

ABSTRACT: Mutational analysis has previously indicated that D83 and E98 residues are essential for DNA cleavage activity and presumably chelate a Mg^{2+} ion at the active site of *Mun*I restriction enzyme. In the absence of metal ions, protonation of an ionizable residue with a pK_a > 7.0, most likely one of the active site carboxylates, controls the DNA binding specificity of *Mun*I [Lagunavicius, A., Grazulis, S., Balciunaite, E., Vainius, D., and Siksnys, V. (1997) *Biochemistry 36*, 11093−11099.]. Thus, competition between H^+ and Mg^{2+} binding at the active site of *Mun*I presumably plays an important role in catalysis/binding. In the present study we have identified elementary steps and intermediates in the reaction pathway of plasmid DNA cleavage by *Mun*I and elucidated the effect of pH and Mg^{2+} ions on the individual steps of the DNA cleavage reaction. The kinetic analysis indicated that the multiple-turnover rate of plasmid cleavage by *Mun*I is limited by product release throughout the pH range 6.0−9.3. Quenched-flow experiments revealed that open circle DNA is an obligatory intermediate in the reaction pathway. Under optimal reaction conditions, open circle DNA remains bound to the *Mun*I; however it is released into the solution at low [$MgCl_2$]. Rate constants for the phoshodiester bond hydrolysis of the first (k_1) and second (k_2) strand of plasmid DNA at pH 7.0 and 10 mM $MgCl_2$ more than 100-fold exceed the k_{cat} value which is limited by product dissociation. The analysis of the pH and [Mg^{2+}] dependences of k_1 and k_2 revealed that both H^+ and Mg^{2+} ions compete for the binding to the same residue at the active site of *Mun*I. Thus, the decreased rate of phosphodiester hydrolysis by *Mun*I at pH < 7.0 may be due to the reduction of affinity for the Mg^{2+} binding at the active site. Kinetic analysis of DNA cleavage by *Mun*I yielded estimates for the association−dissociation rate constants of enzyme−substrate complex and demonstrated the decreased stability of the *Mun*I−DNA complex at pH values above 8.0.

The *Mun*I restriction endonuclease recognizes the hexanucleotide DNA sequence 5′-C↓AATTG-3′ and cleaves it as indicated by the arrow (*1*). The central part of this sequence is identical to the recognition sequence of *Eco*RI (5′-G↓AATTC-3′), which is one of the best-studied restriction enzymes to date (*2*). The discovery of weak protein sequence similarities between *Mun*I and *Eco*RI restriction enzymes (*3*) boosted our interest in molecular mechanisms of sequence discrimination and catalysis by *Mun*I. Mutational analysis of *Mun*I (*4*) guided by sequence alignment between *Mun*I and *Eco*RI indicated that carboxylate residues D83 and E98 are important for DNA cleavage activity and presumably chelate the metal ion at the active site of *Mun*I, similarly to the D91 and E111 residues in *Eco*RI. DNA binding studies surprisingly revealed that, in addition to the proposed role in metal coordination, the carboxylate residue(s) D83 and E98 control DNA binding specificity of *Mun*I in the absence of metal ions (*5*). Indeed, at pH 8.3, at which carboxylate groups would be expected to be completely ionized, *Mun*I exhibited little sequence specificity in DNA binding. Elimination of these carboxylate residues by exchange to alanine or by lowering the pH to 6.5 induced specific DNA recognition by *Mun*I. On the basis of these DNA binding studies it has been suggested that carboxylate residue(s) at the active site of *Mun*I have an anomalously high pK_a value (*5*).

Usually, the pK_a value of carboxylate groups in proteins is between 4 and 5 (*6*), and at physiological pH values, these residues are completely ionized. The negatively charged side chains of acidic amino acid residues often provide an environment that tethers metal cofactors at the active site of enzymes (*7*). The presence of the acidic residue with a perturbed pK_a value at the active site of *Mun*I, however, creates an obvious problem. The metal binding site of *Mun*I should be deprotonated to chelate the metal ion; however an ionized carboxylate residue is likely to interfere with DNA binding specificity. At pH values above the pK_a of the carboxylate residues, chelation of the metal ion at the active site probably resolves this dichotomy. Metal ion binding neutralizes the negative charge at the active site and induces DNA binding specificity of *Mun*I. Indeed, Ca^{2+} ions that do not support cleavage stimulate specific DNA binding by

† This work has been supported in part by NATO Linkage Grant No. 960928, by Volkswagen Stiftung, and by the Deutsche Forschungemeinschaft (Pi 122/12-2).

* To whom all correspondence should be addressed. Fax: 370-2-642624. Tel: 370-2-642404. E-mail: siksnys@ibt.lt.

‡ Institute of Biotechnology.

§ Justus-Liebig-Universitaet.

10.1021/bi982456n CCC: $18.00
Published on Web 03/11/1999

*Mun*I at pH 8.3 (*5*). At pH values close to or below the pK_a, protonation of the active site carboxylate should interfere with metal ion binding. Since Mg^{2+} ion binding is a necessary prerequisite for catalysis to occur, competition between proton and Mg^{2+} for the metal chelating carboxylate at the active site might affect the rate of phosphodiester bond cleavage.

The purpose of the present study was to identify elementary steps and intermediates in the reaction pathway of plasmid DNA cleavage by *Mun*I and to elucidate how individual reaction steps are affected by pH and Mg^{2+} ions. Here we present steady-state and pre-steady-state kinetic analyses of plasmid DNA cleavage by *Mun*I under different conditions. The results of these studies have revealed the limiting step in the steady-state turnover of plasmid DNA cleavage by *Mun*I, have identified reaction intermediates, and have demonstrated that protonation of the active site residues dramatically affects the affinity of Mg^{2+} binding at the active site of *Mun*I.

EXPERIMENTAL PROCEDURES

Protein Purification. Purification of *Mun*I protein was performed as described recently (*4*). The protein was >99% homogeneous as judged by SDS[1] gel analysis. The *Mun*I protein was stored at −20 °C in 10 mM Tris/HCl (pH 7.4, 25 °C), 100 mM KCl, 1 mM EDTA, 1 mM DTT, and 50% glycerol. Protein concentrations were determined by OD_{280} using an extinction coefficient of 45720 M^{-1} cm^{-1} calculated from the amino acid composition. The *Mun*I concentrations are given in terms of the dimeric protein.

Plasmids and DNA. A supercoiled 5.0 kbp pUCGK-4 plasmid (provided by G. Kruckas, MBI "Fermentas") containing a single copy of the recognition sequence of *Mun*I was used as a substrate in this study. Supercoiled pUCGK-4 was isolated from *Escherichia coli* DH5α strain and purified twice by CsCl centrifugation. The amount of supercoiled form in the pUCGK-4 preparation was >90%. The concentration of plasmid DNA was determined by OD_{260} using an extinction coefficient of 67×10^6 M^{-1} cm^{-1}.

A mixture of linear and open circle (nicked specifically at the *Mun*I site) pUCGK-4 was obtained by incubating a 10 nM solution of supercoiled pUCGK-4 with 3 nM *Mun*I for 120 min (pH 8.5, 0.01 mM $MgCl_2$, 37 °C). The final mixture consisted of 60% of the open circle form and 40% of linear DNA. *Mun*I was removed by phenol/chloroform extraction followed by 2-propanol precipitation. Plasmid pUC18 lacking the recognition sequence of *Mun*I under the same reaction conditions remained uncleaved, suggesting that during pUCGK-4 cleavage by *Mun*I single and double strand breaks were only introduced at the *Mun*I recognition sites. The mixture of open circle and linear pUCGK-4 was used as a substrate for the cleavage studies of the open circle form of pUCGK-4 by *Mun*I. The linear form of pUCGK-4, initially present in the reaction mixture presumably did not affect the cleavage rate of the open circle form, since similar amounts of linear DNA had no effect on the cleavage rate of the supercoiled form of pUCGK-4 under similar reaction conditions.

Steady-State Cleavage of pUCGK-4 by MunI. Cleavage experiments were performed at 25 °C in the reaction buffer consisting of 10 mM MES/NaOH (pH 5.5−6.5), 10 mM Tris/HCl (pH 7.0−9.0), or 10 mM Gly/NaOH (pH 9.0−9.5), 50 mM NaCl, and 0.1 mg/ml BSA. Reaction mixtures typically contained 1.5 nM supercoiled pUCGK-4, 0.1−10 mM $MgCl_2$, and 0.15 nM *Mun*I in the reaction buffer with appropriate pH value. Aliquots were removed after fixed time intervals, the reaction stopped by adding $^1/_4$ volume of loading dye solution containing EDTA (50 mM EDTA, pH 8.0, 0.1% SDS, 50% glycerol, 0.01% bromphenol blue) and analyzed by agarose electrophoresis. The amount of supercoiled (SC), open circle (OC), and linear (L) DNA forms was evaluated by densitometric analysis of ethidium bromide-stained gels using software provided by Ultra-Lum. Supercoiled DNA binds less ethidium bromide than relaxed or linear DNA; however separate calibration experiments indicated that in our case the difference in the amounts of supercoiled and linear DNA forms obtained from densitometric analysis was sufficiently small (10−13%) to be neglected. The reaction rates were determined from the linear parts of the reaction progress curves by linear regression.

Quenched-Flow Experiments. An SFM3/Q quenched-flow device (Bio − Logic, Claix) was used to mix 100 μL of a solution containing 1.5 nM pUCGK-4 DNA, 2.4 nM wild-type *Mun*I, and 0.1 mM EDTA in the reaction buffer (10 mM MES/NaOH or 10 mM Tris/HCl, 50 mM NaCl, 0.1 mg/mL BSA) with 100 μL of a solution containing $MgCl_2$ in the same reaction buffer at 25 °C. After appropriate time intervals (50 ms−30 s) the reaction was quenched by mixing with 200 μL of 50 mM EDTA solution (*8*). The DNA was precipitated with ethanol, resuspended in Tris-EDTA buffer, and analyzed by agarose gel electrophoresis. The amounts of different DNA forms were quantitated by densitometric analysis of ethidium bromide-stained gels.

The Effect of the Mixing Procedure on the Cleavage Rate of pUCGK-4 Plasmid DNA by MunI. Reaction of pUCGK-4 cleavage was initiated by 3 different procedures: (i) adding $MgCl_2$ solution to the premixed *Mun*I−pUCGK-4 solution, (ii) adding DNA solution to the *Mun*I solution containing $MgCl_2$, and (iii) adding the *Mun*I solution to the DNA solution containing $MgCl_2$. The concentrations of *Mun*I, pUCGK-4, and $MgCl_2$ in the final reaction mixture were always the same. Samples were removed after fixed time intervals and analyzed as described above. Cleavage of the open circle form of pUCGK-4 specifically nicked at the *Mun*I site was studied in a similar way except that 0.9 nM substrate instead of 1.5 nM was used in the final reaction mixture. All of these experiments were performed at sufficiently low $MgCl_2$ concentrations that enabled one to follow the reaction using a manual mixing technique. The shortest accessible time in such experiments was 4 ± 1 s.

Data Analysis and Curve Fitting. Values of reaction rate constants, corresponding to the separate steps of plasmid DNA cleavage by *Mun*I (eqs 3, 6, 7), were obtained by nonlinear regression using the Excel (Microsoft) "solver" option to minimize the sum of squared differences between calculated and experimental data values (*8*). The theoretical values for various substrate forms were calculated from the

[1] Abbreviations: bp, base pair(s); EDTA, ethylenediaminetetraacetic acid; PAAG, polyacrylamide gel; SDS, sodium dodecyl sulfate; DTT, dithiothreitol; Tris, tris(hydroxymethyl)aminomethane; SC, supercoiled plasmid DNA; OC, open circle plasmid DNA; L, linear DNA; E, enzyme.

integrated rate equations, describing the corresponding reaction. In the case of eq 3, analytical solutions of rate equations were used, while in the case of more complex reaction pathways (eqs 6, 7), theoretical values for all substrate forms were obtained by numerical calculations. The reaction pathways, represented by eqs 6 and 7, contain four and six rate constants, respectively, and their values could not be determined from a single time course of plasmid DNA cleavage. Therefore, calculated theoretical values for all substrate forms were simultaneously fitted to the experimental data sets, obtained at various enzyme concentrations with the different mixing procedures of the reaction components, yielding a single set of rate constants. For example, numerical solutions of differential equations corresponding to scheme 6 were simultaneously fitted to the time courses of supercoiled plasmid cleavage, obtained at fixed pH, [$MgCl_2$], four different enzyme concentrations (1.1, 2.2, 4.5, and 9 nM), and two different mixing procedures of the reaction components (reactions were initiated either from preincubated or separate enzyme and DNA solutions) at each enzyme concentration. Different reaction components' mixing procedures were taken into account during numerical integration by setting different initial concentrations of enzyme, substrate, and corresponding enzyme−substrate complex. In the case of the reaction start from separate enzyme and DNA solutions, the initial concentration of enzyme−substrate complex was set equal to 0. If the reaction was started from preincubated enzyme−DNA solution, the initial concentration of the enzyme−substrate complex was calculated from the corresponding enzyme−specific DNA association equilibrium. A wide variety of data, simultaneously used in the fitting procedures, made the minimized sum of squared residuals sensitive to the changes of all rate constants considered.

RESULTS AND DISCUSSION

Cleavage of pUCGK-4 by MunI under Steady-State Conditions. Initially, cleavage of supercoiled pUCGK-4 by *Mun*I was studied in multiple-turnover kinetic experiments with limiting enzyme (0.15 nM) and an excess of substrate (1.5 nM). Under these conditions the enzyme must perform a number of catalytic cycles in order to achieve complete cleavage of substrate DNA. Analysis of the time course of DNA hydrolysis by *Mun*I at pH 7.0, 10 mM $MgCl_2$, and 25 °C revealed a small but steep decline of SC DNA concentration over the first 100 s of the reaction followed by a linear steady-state phase (Figure 1). Such a reaction profile is consistent with product burst kinetics (*9*). The reaction rates corresponding to the linear phase of the reaction progress curves increased with increasing *Mun*I concentration (data not shown) and were invariant across the range of substrate concentrations (1−10 nM) throughout the pH interval 6.0−9.0 as expected for an enzymatic reaction under steady-state conditions at saturating substrate concentrations. The reaction rate determined from the slope of the linear steady-state phase was therefore treated as v_{max}. The k_{cat} value of 0.15 ± 0.01 min^{-1} (pH 7.0, 10 mM Mg^{2+}, 25 °C) was obtained from the data presented in Figure 1. Noteworthy, the amount of OC DNA remained constant during the reaction and did not exceed the background level (Figure 1), which is indicative of a concerted double strand cleavage. Analysis of supercoiled pUCGK-4 cleavage at varying *Mun*I concentrations

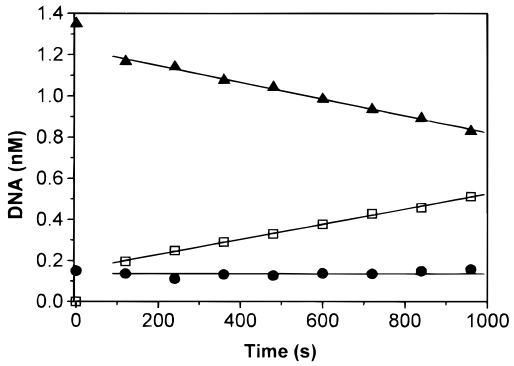

FIGURE 1: Steady-state cleavage of supercoiled pUCGK-4 by *Mun*I. The reaction mixture contained 1.5 nM pUCGK-4, 0.15 nM *Mun*I, 10 mM $MgCl_2$, 10 mM Tris/HCl, pH 7.0, 50 mM NaCl, and 0.1 mg/mL BSA at 25 °C. Concentrations of supercoiled (▲), linear (□), and open circle (●) forms of pUCGK-4 are shown. Solid lines were obtained by linear regression in the time interval between 100 and 960 s.

(still maintaining the substrate concentration in excess) revealed that, in accordance with the product burst kinetics, the amount of the substrate cleaved during the fast phase was proportional to the concentration of enzyme (data not shown). The concentration of *Mun*I determined from the burst amplitude corresponded to approximately 80% of the enzyme active sites in the experiment. Hence, all of these data indicate that the product release is the slowest step of plasmid DNA cleavage by *Mun*I under the multiple-turnover conditions. The steady-state rate constant k_{cat}, obtained from the linear phase of time course of product accumulation, corresponds therefore to the rate of the product (linear DNA) dissociation.

Rate-limiting product release under steady-state conditions has been reported for the *Eco*RI (*10*), *Eco*RV (*11*), *Nae*I (*12*), and *Sfi*I (*13*) restriction enzymes. The k_{cat} values for macromolecular DNA cleavage by *Eco*RI (*10*) and *Eco*RV (*11*) were similar to that obtained for *Mun*I under similar reaction conditions (pH 7.0, 10 mM Mg^{2+}, 25 °C). Earlier kinetic studies of *Cla*I, *Xar*II, and *Sma*I restriction enzymes also suggest that product dissociation might be a rate-limiting step during plasmid DNA cleavage under multiple-turnover conditions (*14*). Hence, rate-limiting product release might be a general feature for the cleavage of macromolecular DNA by restriction enzymes under steady-state conditions.

In principle, there are at least two alternative ways for the restriction enzyme being trapped in an enzyme−product complex: it can be transferred to nonspecific sequences after cleavage before dissociating into solution as it was proposed for *Eco*RI (*10, 15*) or it can remain bound to the ends of the DNA, in particular the terminal phosphate(s) after phosphodiester bonds cleavage. In either case protons or/and Mg^{2+} ions can contribute to the stability of the enzyme−product complex. Thus, the role of Mg^{2+} ions and pH on the k_{cat} for pUCGK-4 plasmid cleavage by *Mun*I has been studied.

The Mg^{2+} dependence of k_{cat} at pH 8.0 is displayed in Figure 2. Variation of $MgCl_2$ concentration from 1 to 10 mM resulted in a 1.5-fold increase of k_{cat} for pUCGK-4 cleavage by *Mun*I (Figure 2). Strikingly, at $MgCl_2$ concentrations below 1.0 mM, the k_{cat} value increases with decreasing $MgCl_2$ concentration. The k_{cat} value (0.01 s^{-1}) obtained at 0.1 mM $MgCl_2$ was twice that of the value (0.005 s^{-1})

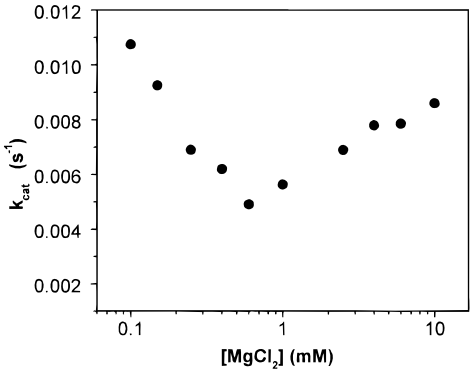

FIGURE 2: $MgCl_2$ concentration dependence of k_{cat}. The reaction mixtures contained 10 mM Tris/HCl, pH 8.0, 50 mM NaCl, 0.1 mg/mL BSA, 0.15 nM *Mun*I, 1.5 nM pUCGK-4, and 0.1−10 mM $MgCl_2$ at 25 °C. k_{cat} values (●) were calculated from steady-state experiments using linear regression.

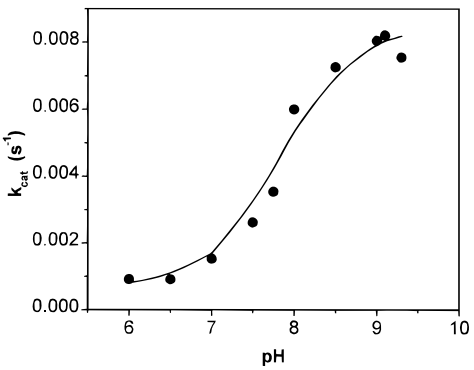

FIGURE 3: Dependence of k_{cat} on pH. The reaction mixtures contained 1 mM $MgCl_2$, 1.5 nM pUCGK-4, 0.15 nM wild-type *Mun*I, 0.1 mg/mL BSA, 10 mM Tris/HCl, Mes/NaOH or Gly/NaOH, and 50 mM NaCl at 25 °C. k_{cat} values (●) were calculated from steady-state experiments using linear regression. Solid lines represent the optimal fit of the data to eq 2 with parameters $pK_a = 7.8 \pm 0.2$, $k_{diss}^{ELH} = 0.0006 \pm 0.0004$ s^{-1} and $k_{diss}^{EL} = 0.0080 \pm 0.0005$ s^{-1}.

determined at 1.0 mM $MgCl_2$. It should be noted that, across the range of $MgCl_2$ concentrations tested (0.1−10 mM), product DNA accumulation curves remain biphasic (similar to those presented in Figure 1). At $MgCl_2$ concentrations below 0.1 mM, the burst phase became less pronounced, suggesting that the rate difference between product release and preceding steps is getting smaller. A Mg^{2+} dependence qualitatively similar to that presented in Figure 2 has been obtained at pH 7.0 (data not shown). The increase of k_{cat} with $MgCl_2$ concentration above 1 mM is probably due to the ionic strength effect since a similar rate increase has been observed at 1 mM $MgCl_2$ when additional 27 mM NaCl was added to the reaction buffer to keep the ionic strength constant at 1 and 10 mM of $MgCl_2$ (data not shown). We suppose that at pH 8.0 and [$MgCl_2$] > 1mM, Mg^{2+} ions still remain bound to the enzyme−product complex after DNA cleavage and probably retard product dissociation. The increase of salt concentration facilitates the breakdown of the complex and product release. At [$MgCl_2$] < 1mM, the enzyme−product complex is probably not saturated with Mg^{2+} ions, and therefore, product dissociation rate (k_{cat}) is increased.

If a prototropic equilibrium is involved in a product dissociation step, pH should affect the steady-state rate. Therefore, the pH dependence of k_{cat} for pUCGK-4 cleavage by *Mun*I has been studied under steady-state conditions in the pH range of 6.0−9.3 at 1 mM $MgCl_2$. At all pH values tested reaction progress curves for product accumulation were biphasic (similar to those in Figure 1), suggesting that there is no change of the rate-limiting step with pH and that product dissociation still limits the steady-state rates throughout the pH range 6.0−9.3. At higher pH values, the dissociation-limited rate constant could not be determined due to the decreased enzyme stability. The k_{cat} values at all pH values were calculated from the slopes of the linear phase similarly as described for the data presented in Figure 1. The pH dependence of k_{cat} for plasmid DNA cleavage by *Mun*I is displayed in Figure 3. If we assume that single proton binding affects the product dissociation rate, eq 1 can be applied for the analysis of the pH dependence of k_{cat} for pUCGK-4 cleavage by *Mun*I:

$$\begin{array}{ccc} & k_{diss}^{EL} & \\ E{\cdot}L & \rightarrow & E + L \\ & + & \\ & H^+ & \\ K_a & \updownarrow & \\ E{\cdot}L{\cdot}H^+ & \rightarrow & E{\cdot}H^+ + L \\ & k_{diss}^{ELH} & \end{array} \qquad (1)$$

where k_{diss}^{EL} and k_{diss}^{ELH} are dissociation constants for deprotonated and protonated forms of the enzyme−product complex, respectively, and K_a is the equilibrium dissociation constant. The pH dependence of k_{cat} is then described by eq 2:

$$k_{cat} = k_{diss}^{ELH}[H^+]/([H^+] + K_a) + k_{diss}^{EL}K_a/([H^+] + K_a) \quad (2)$$

Fitting eq 2 to the data of Figure 3 yielded estimated values for $k_{diss}^{ELH} = 0.0006 \pm 0.0004$ s^{-1}, $k_{diss}^{EL} = 0.0080 \pm 0.0005$ s^{-1}, and $pK_a = 7.8 \pm 0.2$, respectively. Thus, the dissociation rate constant of the deprotonated form is 10-fold higher than that of the protonated form. The interpretation of the pH dependence of k_{cat} is relatively straightforward if one assumes that protonation−deprotonation of particular residues at the active site with an apparent $pK_a \approx 7.8$ controls the product dissociation rate. Several amino acid side chains with ionizable groups with pK_a close to 7.0−8.0 are probably adjacent to the active site. It is impossible to identify such groups in the absence of a high-resolution X-ray structure; however indirect evidence allows us to speculate about the involvement of two possible candidates. DNA binding studies with *Mun*I have suggested (*5*) that active site carboxylate residues exhibit pK_a values between 7.0 and 8.0. Alternatively, terminal phosphate residues might be considered as possible candidates. During the cleavage reaction, the monoionic phosphodiester of the scissile bond is transformed to a dianionic 5′-monophosphate. The pK_a values of the dibasic monophosphate group are 1.0 and 6.6 (*16*). The presence of adjacent negatively charged residues, for example, active site carboxylates, in the *Mun*I−product complex might cause an upward shift of the pK_a value of the terminal phosphate residue (*17*). Hence, protonated carboxylate or terminal phosphate residues might strengthen enzyme−product interactions (e.g., through a shared hydrogen bond)

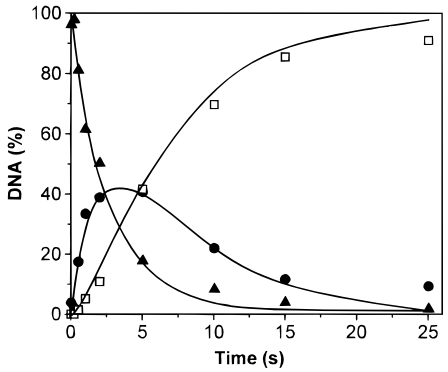

FIGURE 4: Quench-flow experiment of supercoiled pUCGK-4 cleavage by *Mun*I under single-turnover conditions. The reaction was started by mixing equal volumes of a solution containing pUCGK-4 and *Mun*I in reaction buffer (10 mM Tris/HCl pH 7.0, 50 mM NaCl, 0.1 mg/mL BSA) with a separate solution of $MgCl_2$ in the same buffer at 25 °C. The final solution contained 0.75 nM pUCGK-4, 1.2 nM *Mun*I, and 2.5 mM $MgCl_2$. The time course of the amount of supercoiled (▲), open circle (●), and linear (□) DNA is displayed. Solid lines represent the optimal fit of the data to eq 3 with parameters $k_1 = 0.44\ s^{-1}$ and $k_2 = 0.20\ s^{-1}$.

and reduce product dissociation rates. However, even at pH values above the pK_a of a putative active site residue, the k_{cat} for pUCGK-4 cleavage by *Mun*I is still limited by product dissociation. We suppose that, after deprotonation of the active site, bridging of Mg^{2+} ions between the ionized terminal phosphate and enzyme active site residues might retard product liberation from the active site, similar to proton binding at pH values below pK_a. Indeed, an increased rate of product dissociation has been observed at pH values between 8.0 and 9.3 and $MgCl_2$ concentrations below 1.0 mM (Figure 2): under these conditions, the enzyme−product complex presumably is not saturated by Mg^{2+} ions and product release is fast as compared to the situation at higher Mg^{2+} concentrations (1 mM). Indirect supportive evidence for this interpretation comes from crystallographic studies of the *Eco*RV−product complex (*18*). Two Mg^{2+} ions were found to be bound to the terminal phosphate in the *Eco*RV−product complex, while only a single Mg^{2+} ion was present in the *Eco*RV−substrate complex. Moreover, one of the Mg^{2+} ions in the *Eco*RV−product complex bridges active site carboxylate residues and phosphate termini (*18*). However, it must be demonstrated directly by further biochemical and structural studies if *Mun*I remains associated with the terminal phosphate residue after cleavage.

Pre-Steady-State Studies of pUCGK-4 Plasmid Cleavage by MunI Restriction Endonuclease. The burst phase rates corresponding to the first turnover of plasmid DNA cleavage by *Mun*I might be limited by the rate of phosphodiester bond hydrolysis or alternatively by earlier steps preceding the hydrolytic step, for example, enzyme isomerization or DNA binding. To get more insights into the pre-steady-state cleavage of plasmid DNA, single-turnover experiments were conducted using a rapid-quench technique (*19*). The reaction was carried out by mixing a solution of pUCGK-4 (1.5 nM) and *Mun*I (2.4 nM) contained in one syringe with a $MgCl_2$ solution in another syringe and quenched after different time intervals by the addition of EDTA (see Experimental Procedures). A representative time course of SC plasmid DNA cleavage by *Mun*I (pH 7.0, 2.5 mM $MgCl_2$, 25 °C) is shown in Figure 4. The observed reaction pattern is suggestive of a sequential reaction pathway in which the *Mun*I first cuts one DNA strand converting the supercoiled DNA to open circle, and then the second strand to yield a linear product. A sequential pathway of plasmid DNA cleavage has been already reported for *Eco*RI (*10*), *Eco*RV (*20*), *Bam*HI (*21*), *Taq*I (*22*), *Cfr*9I (*23*), and *Sfi*I (*13*) restriction enzymes.

Cleavage rates of pUCGK-4 plasmid by *Mun*I under single-turnover conditions were invariant with excess enzyme concentration across the pH range 5.5−8.0 (data not shown). Scheme 3 has been applied for the analysis of the data in Figure 4:

$$E{\cdot}SC \xrightarrow{k_1} E{\cdot}OC \xrightarrow{k_2} E{\cdot}L \qquad (3)$$

where k_1 and k_2 are the first-order rate constants for the cleavage of the first and the second DNA strands, respectively. Nonlinear regression analysis (see Experimental Procedures) yielded values of 0.44 and 0.2 s^{-1} for the rate constants k_1 and k_2, respectively. If the cleavages of both substrate DNA strands by the restriction enzyme are independent events k_1 should be twice the value of k_2 due to the 2-fold higher probability of forming the OC form from SC plasmid than forming linear DNA from OC plasmid (*24*). Indeed, in the case of pUCGK-4 cleavage by *Mun*I, k_1 is equal to $2k_2$.

Mg^{2+} is a necessary cofactor for DNA cleavage by *Mun*I restriction endonuclease. To test the role of Mg^{2+} ions on the single-turnover rates of pUCGK-4 cleavage by *Mun*I, we performed a set of quenched-flow experiments at different pH values (6.5−8.0) and varying $MgCl_2$ concentrations (0.1−10 mM). In all experiments $MgCl_2$ solution was added to the premixed *Mun*I−DNA complex and *Mun*I concentrations were saturating. Under suboptimal reaction conditions (pH 5.5 and 6.0 and at pH > 6.0 and [$MgCl_2$] < 2.0 mM), the single turnover of pUCGK-4 cleavage is slow enough to follow the reaction by manual mixing of *Mun*I−DNA and $MgCl_2$ solutions. At all pH and $MgCl_2$ concentrations tested reaction profiles were qualitatively similar to those shown in Figure 4, suggesting that the reaction of plasmid DNA cleavage by *Mun*I follows the sequential pathway (eq 3). Therefore, a similar fitting routine has been applied to obtain values of k_1 and k_2 at different pH and varying $MgCl_2$ concentrations. The Mg^{2+} dependence for reaction rate constant k_1 for the cleavage of pUCGK-4 by *Mun*I under single-turnover conditions is displayed in Figure 5. Similar Mg^{2+} dependences were obtained for k_2 (data not shown). Under all experimental conditions, the value of k_1 approximately exceeded the value of k_2 by a factor of 2.

The Mg^{2+} dependences of the k_1 and k_2 values were qualitatively different at different pH values (Figure 5). At pH values above 7.0, saturation with Mg^{2+} is achieved, while at pH values below 6.5, k_1 values increase linearly with increasing $MgCl_2$ concentration over the entire range (0.1−10 mM) tested. We suppose that the increase of the DNA cleavage rate with increasing $MgCl_2$ concentration observed at pH > 7.0 is due to the progressive saturation of the *Mun*I active sites with Mg^{2+}. Then eq 4 should describe the Mg^{2+} dependences of k_1 and k_2 at fixed pH values:

$$k = k_{max}[Mg^{2+}]/(K_{Mg} + [Mg^{2+}]) \qquad (4)$$

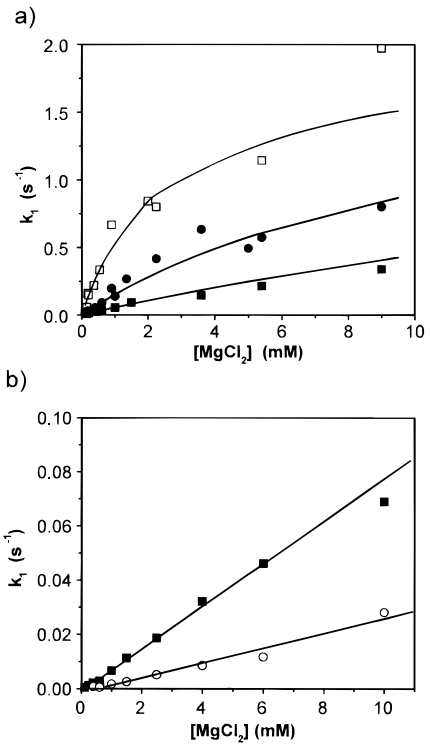

FIGURE 5: $MgCl_2$ concentration dependence of the rate constant k_1 for the cleavage of the first strand of the supercoiled form of pUCGK-4. Reactions were performed at 25 °C at different pH values and $MgCl_2$ concentrations, and data were analyzed as in Figure 4. (a) k_1 values at pH 8.0 (□), pH 7.0 (●), pH 6.5 (■). Solid lines represent the optimal fit of the experimental data to eq 5 with parameters $pK_a^1 = 7.8 \pm 0.2$, $K_{Mg}^1 = 1.5 \pm 0.5$ mM, and $k_{max}^1 = 1.9 \pm 0.2$ s^{-1}. (b) k_1 values at pH 6.0 (■) and pH 5.5 (○). Solid lines represent linear fits to the data.

where k is a single-turnover rate constant for the first or second DNA strand cleavage by *Mun*I, k_{max} is the rate constant at saturating $MgCl_2$ concentration and fixed pH, and K_{Mg} is the equilibrium constant for Mg^{2+} dissociation from E·SC or E·OC. According to eq 4, at $K_{Mg} \leq [Mg^{2+}]$, the dependence of k_1 should exhibit a hyperbolic dependence on $MgCl_2$ concentration. Indeed, such a dependence is observed at pH 8.0 for k_1 (Figure 5a). If $K_{Mg} \gg [Mg^{2+}]$, according to eq 4, k_1 and k_2 depend linearly on the Mg^{2+} concentration. Linear dependence of k_1 on Mg^{2+} concentration is observed at pH 5.5 and 6.0 (Figure 5b). Thus, experimental data presented in Figure 5b suggest that at pH $\leq$ 6.0 the active site of *Mun*I is not saturated with Mg^{2+} ions even at the highest $MgCl_2$ concentration tested (10 mM); however saturation is achieved at higher pH values (Figure 5a). If one assumes that only Mg^{2+}−enzyme−substrate complexes are productive and if H^+ and Mg^{2+} ions compete for the same binding site in the *Mun*I−substrate complex, eq 5, qualitatively similar to the equation for competitive inhibition of enzymatic reactions, should describe the data in Figure 5:

$$k = k_{max}[Mg^{2+}]/[K_{Mg}(1 + [H^+]/K_a) + [Mg^{2+}]] \quad (5)$$

where k is a single-turnover rate constant for the first or the second DNA strand cleavage by *Mun*I, k_{max} is the rate constant value at saturating Mg^{2+} concentration, K_{Mg} is the equilibrium constant for Mg^{2+} dissociation from E·SC or E·OC, and K_a is the equilibrium constant for deprotonation of an acidic residue. The solid lines in Figure 5 (panel a) were obtained by fitting eq 5 to the experimental data for k_1. The fitting routine yielded the following optimal values of the individual parameters: $pK_a^1 = 7.8 \pm 0.2$, $K_{Mg}^1 = 1.5 \pm 0.5$ mM, $k_{max}^1 = 1.9 \pm 0.2$ s^{-1}. Equation 5 satisfactorily describes the experimental data. Thus, the analysis of the pH dependences of Mg^{2+} binding by *Mun*I supports the assumption that Mg^{2+} and H^+ ions compete for the binding to the same residue(s) at the active site of *Mun*I. Noteworthy, values of phosphodiester bond cleavage rate constants k_1 and k_2 determined for *Mun*I were close to those reported for *Eco*RI (*10*), *Bam*HI (*25*), *Eco*RV (*20*, *24*), and *Taq*I (*22*). However, for the latter enzymes Mg^{2+} dependences of k_1 and k_2 at different pH values were not determined. It would be interesting to see if the subtle interplay between Mg^{2+} and H^+ binding at the active site of *Mun*I is also important in the regulation of cleavage activity/binding specificity of other restriction enzymes.

The results of site-directed mutagenesis experiments suggest that D83 and E98 carboxylate residues chelate Mg^{2+} at the active site of *Mun*I. It was supposed (*5*) that active site carboxylate residue(s) of *Mun*I exhibit anomalously high pK_a values (above 7.0) and protonation of this residue affects DNA binding specificity of *Mun*I in the absence of divalent metal ions. At pH below 7.0, carboxylate residues become protonated and this stimulates formation of the tight sequence-specific complex between *Mun*I and DNA. However, if H^+ and Mg^{2+} compete for the same carboxylate residues, protonation at pH below 7.0 will interfere with effective binding of Mg^{2+} at the active site and should reduce DNA cleavage activity of *Mun*I. At high pH values, active site residues are deprotonated and effectively bind divalent metal ions. Deprotonation of active site residues reduces DNA binding affinity of *Mun*I in the absence of Mg^{2+} ions. However, effective binding of Mg^{2+} at the active site compensates for the loss of a proton at the active site because metal ion binding decreases the negative charge at the active site and presumably increases complex stability similarly as proton binding at lower pH. Increased DNA binding affinity of *Mun*I at pH 8.0 in the presence of Ca^{2+} ions supports this assumption (*5*). It is tempting to speculate that both H^+ and metal ions at the active site of *Mun*I perform a similar function with respect to DNA binding by increasing protein−DNA complex stability; however, only chelation of Mg^{2+} at the active site supports catalysis. Binding of Mg^{2+} ions probably stabilizes the transition state of the reaction enabling catalysis while the effects of Ca^{2+} ions and H^+ are mainly manifested at the ground state.

Carboxylate residues are often involved in chelation of metal ions at the active sites of metal ion-dependent enzymes involved in hydrolysis of nucleic acids and phosphoryl transfer. Interestingly, anomalous pK_a values of carboxylate residues coordinating Mg^{2+} ions at the active sites have been reported in the literature. A carboxylate residue involved in chelation of Mg^{2+} ion at the active site of CheY protein exhibits an increased pK_a value (*26*). Analysis of heteronuclear two-dimensional NMR titration experiments with RNaseH revealed that the Asp10 carboxylate at the active site has an anomalously high pK_a value of 6.1 (*27*).

In the quenched-flow experiments described above the reaction was initiated by rapid mixing of a preincubated *Mun*I−pUCGK-4 solution with a $MgCl_2$ solution. If slow

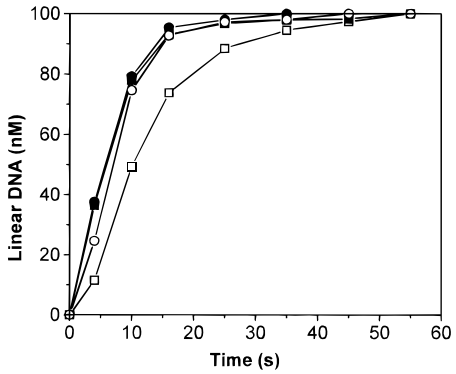

FIGURE 6: Mixing order dependence of the rate of formation of linear DNA. Experiments were performed at pH 7.0, with 5 mM $MgCl_2$ and 1.5 nM pUCGK-4 and using a manual mixing technique. Solid symbols correspond to reactions started by adding $MgCl_2$ solution to the preincubated *Mun*I−pUCGK-4 solution. Open symbols correspond to reactions performed by mixing a solution containing *Mun*I and $MgCl_2$ with a separate solution containing pUCGK-4. Data represented by squares (■, □) refer to 2.2 nM *Mun*I, and data represented by circles (●, ○) refer to 9 nM *Mun*I.

conformational rearrangements do not accompany Mg^{2+} binding to the pre-equilibrated *Mun*I−pUCGK-4 complex, single-turnover rates observed under these conditions refer to the chemical step of phosphodiester bond cleavage. However, if the reaction is initiated by mixing separate *Mun*I and pUCGK-4 solutions, rates of binding of enzyme to DNA or monomolecular conformational changes might become rate-limiting. To examine this possibility, we studied pUCGK-4 cleavage by *Mun*I under pre-steady reaction conditions (with enzyme equal or in excess over substrate) starting the reactions from preincubated *Mun*I−pUCGK-4 solution or separate *Mun*I and pUCGK-4 solutions.

Indeed, at pH 7.0 slower rates of linear DNA accumulation were observed in the reactions, started by mixing separate *Mun*I and pUCGK-4 solutions rather than in the reactions initiated from the preincubated *Mun*I−pUCGK-4 solution (Figure 6). Moreover, while in the case of preincubated *Mun*I−pUCGK-4 solution, cleavage rates were invariant with enzyme concentration, the cleavage rates in the reactions started from separate *Mun*I and pUCGK-4 solutions increased with *Mun*I concentration until the reaction rate level observed with preincubated *Mun*I and pUCGK-4 solutions is reached (Figure 6). Similar reaction patterns were observed at pH 7.5 and 8.0. However, at pH > 8.0 reaction rates became dependent on *Mun*I concentration regardless of the mixing procedure (data not shown).

The enzyme concentration dependence of substrate cleavage rate in principle rules out the possibility that differences in progress curves of product accumulation observed with different mixing modes (Figure 6) are due to the slow conformational rearrangements of enzyme or DNA. Such structural changes should be monomolecular, but the reaction rate dependence on *Mun*I concentration in the reactions initiated from separate enzyme and DNA solutions suggests a bimolecular nature of the process, preceding the phosphodiester bond cleavage. Thus, conformational changes accompanying *Mun*I binding to the cognate DNA (*5*) are probably sufficiently fast in the time scale of the experiments presented here and do not limit the observed rates.

To evaluate association−dissociation rates for the *Mun*I−pUCGK-4 interaction, we used scheme 6:

$$E + SC \underset{k_d^{SC}}{\overset{k_{on}^{SC}}{\rightleftharpoons}} E{\cdot}SC \xrightarrow{k_1} E{\cdot}OC \xrightarrow{k_2} E{\cdot}L \qquad (6)$$

where k_{on}^{SC} is the association rate constant for *Mun*I binding to its recognition sequence, k_d^{SC} is the dissociation rate constant of the specific *Mun*I−DNA complex, respectively, and k_1 and k_2 are rate constants for the phosphodiester bond cleavage. Equation 6 was applied for the analysis of the experimental data obtained at various pH values, enzyme concentrations, and mixing procedures. Optimal values for rate constants k_1, k_2, k_{on}^{SC}, and k_d^{SC} at various pH values were obtained by fitting numerical solutions of differential equations corresponding to eq 6 to the experimental data. It should be pointed out that obtained k_{on}^{SC} and k_d^{SC} values should be treated only as estimates. Values of k_1 and k_2 were very close to those obtained by single-turnover quench-flow experiments at the same pH and [$MgCl_2$] (see, above). The pH dependences of the obtained k_{on}^{SC} and k_d^{SC} are presented in Figure 7. The estimated *Mun*I−DNA association rate constant values k_{on}^{SC} monotonically decrease with pH from the value 3×10^8 M^{-1} s^{-1} at pH 7.0 to the value 2×10^7 M^{-1} s^{-1} at pH 9.0. The dissociation rate constant k_d^{SC} is close to 0 between pH 7 and 7.5 and monotonically increases in the pH range 8.0−9.0 from 0.03 to 0.3 s^{-1} (Figure 7). All experimental data sets used in the analysis of scheme 6 were obtained at low Mg^{2+} concentrations (2−5 mM at pH 7.0, 1−2 mM at pH 7.5, 1 mM at pH 8.0−9.0). Under these conditions, according to eq 5, only a small fraction of the *Mun*I−pUCGK-4 complexes is saturated by Mg^{2+}. Thus, the values for the apparent rate constants k_{on}^{SC} and k_d^{SC} obtained by the fitting routine most likely represent association−dissociation rates of binary (Mg^{2+}-free) *Mun*I−pUCGK-4 complex. The equilibrium dissociation constant K_d values for *Mun*I−pUCGK-4 complex were calculated from the k_d^{SC}/k_{on}^{SC} ratio. The calculated K_d values are ≤0.03 nM at pH 7.0 and 15.0 nM at pH 9.0, respectively. Gel shift analysis of DNA binding by *Mun*I revealed a stable *Mun*I−DNA complex at pH ≤ 7.0; however at pH values above 8.0 it was not detectable in the gel (*5*). The K_d values estimated from the k_d^{SC}/k_{on}^{SC} ratio suggest that the *Mun*I−pUCGK-4 complex exists throughout the pH range 7.0−9.0; however its stability and lifetime decrease with increasing pH. The failure to detect *Mun*I−DNA complexes in gel shift experiments at pH > 8.0 might be due to the increased k_d^{SC} of the *Mun*I−DNA complex. Hence, it is tempting to speculate that ionization of the active site carboxylate residue at pH > 7.0 might cause the increase of k_d^{SC} and destabilize the *Mun*I−DNA complex. Binding of the metal ion at the active site at pH > 7.0 probably increases complex stability. Indeed, stable *Mun*I−DNA complexes are observed at pH 8.3 in the presence of Ca^{2+} (*5*).

During the steady-state cleavage of pUCGK-4 by *Mun*I (Figure 1) the amount of open circle form remains constant and does not exceed the background level. Such a reaction profile is consistent with a concerted DNA cleavage mechanism in which *Mun*I cuts both strands of its recognition sequence during the lifetime of an enzyme−substrate complex. However, at low Mg^{2+} concentrations (0.025 mM) the amount of open circle pUCGK-4 exceeds that of the enzyme by a factor of 3, suggesting that open circle DNA is released into the solution (data not shown). Noteworthy, a similar release of open circle DNA at low Mg^{2+} concentrations has

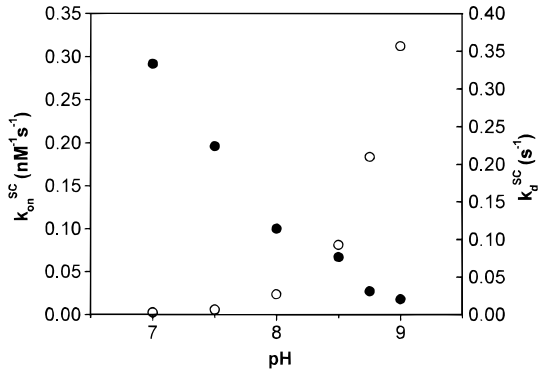

FIGURE 7: pH dependence of the apparent association rate constant k_{on}^{SC} and the dissociation rate constant k_d^{SC} for the *Mun*I−pUCGK-4 interaction. k_{on}^{SC} (●) and k_d^{SC} values (○) were obtained by applying a simultaneous fitting routine to the experimental data sets of plasmid DNA cleavage by *Mun*I obtained at various enzyme concentrations and using different mixing procedures (see Experimental Procedures).

been reported earlier for *Eco*RV (*24*). Under particular reaction conditions supercoiled plasmid pUCGK-4 was converted into the open circle form with high yield (see Experimental Procedures). The obtained open circle DNA was used subsequently as a substrate in the kinetic studies. Equation 7, including the reversible step of open circle substrate dissociation, was used for analysis of the experimental data, obtained for the cleavage of supercoiled and open circle pUCGK-4 forms by *Mun*I (see Experimental Procedures):

$$\begin{array}{ccccc} & k_{on}^{SC} & k_1 & k_2 & \\ E + SC \leftrightarrow & E\cdot SC & \rightarrow E\cdot OC & \rightarrow E\cdot L & \\ & k_d^{SC} & k_d^{OC}\updownarrow k_{on}^{OC} & & \\ & & E + OC & & \end{array} \quad (7)$$

where the rate constants are defined as in eq 6 and k_{on}^{OC} and k_d^{OC} are association and dissociation rate constants of the E·OC complex, respectively. Regression analysis yielded values for six apparent rate constants k_{on}^{SC}, k_d^{SC}, k_1, k_2, k_{on}^{OC}, and k_d^{OC}. The estimated value of 0.04 s^{-1} (pH 7.0, 5.0 mM $MgCl_2$) was obtained for the rate constant k_d^{OC}. If we assume that, at pH 7.0, 5 mM Mg^{2+}, 25 °C, the k_2 value is ~0.3 s^{-1}, than the ratio k_2/k_d^{OC} would be close to seven. This means that only few E·OC complexes dissociate and release OC plasmid before its conversion into linear DNA. Therefore, open circle DNA does not accumulate under steady-state reaction conditions (Figure 1). By lowering the Mg^{2+} concentration, the rate constant k_2 (see eq 5) and the ratio k_2/k_d^{OC} decrease and a much larger fraction of E·OC complexes dissociates which leads to the accumulation of open circle plasmid DNA in solution under steady-state reaction conditions.

CONCLUSIONS

The kinetic analysis of pUCGK-4 cleavage by *Mun*I indicates that product release limits the overall reaction rate under multiple-turnover conditions. The turnover number k_{cat} exhibits a sigmoidal pH dependence: it is independent of pH in the range 6.0−6.5, increases in the pH range 7.0−8.5, and reaches a limiting value at pH > 8.5. Such pH dependence suggests that protonation of the active site residue or of the product affects the rate of product release.

Quenched-flow experiments of plasmid DNA cleavage initiated by adding $MgCl_2$ to the premixed *Mun*I−pUCGK-4 solution revealed that open circle DNA is an obligatory intermediate in the reaction pathway of plasmid DNA cleavage by *Mun*I. Under optimal reaction conditions, open circle DNA remains bound to *Mun*I; however it is released into the solution under suboptimal reaction conditions (low [$MgCl_2$]).

Rate constants for the first (k_1) and the second (k_2) strand cleavage of the closed supercoiled form of pUCGK-4 plasmid referring to the rates of phosphodiester hydrolysis were determined from quenched-flow experiments at saturating *Mun*I concentrations. The pH and Mg^{2+} dependence of k_1 and k_2 reveals that, at pH > 7.0, saturation by Mg^{2+} is achieved; however at pH values below 7.0, both k_1 and k_2 increase linearly with increasing Mg^{2+} concentration. Such Mg^{2+} dependences are consistent with the assumption that both H^+ and Mg^{2+} ions compete for the binding to the same active site carboxylate residue. The lower DNA cleavage activity of *Mun*I at pH < 7.0 is therefore presumably due to the decreased affinity of Mg^{2+} for the active site.

We suppose that ionization of the same active site carboxylate residue(s) determines both the metal and specific DNA binding properties of *Mun*I. At pH < 7.0, protonated carboxylate residue(s) favor formation of the tight sequence-specific complex between *Mun*I and DNA. However, protonation interferes with effective binding of Mg^{2+} at the active site and leads to the decreased DNA cleavage rate. At pH > 7.0, active site residue(s) become deprotonated and effectively chelate metal ion. Chelation of the Mg^{2+} ions at the active site neutralizes the overall negative charge at the active site, increases the stability of the specific complex, and promotes catalysis. Thus, binding of both H^+ and metal ions at the active site of *Mun*I probably increases protein−DNA complex stability by neutralizing the negative charge of the active site carboxylate residue(s). Binding of Mg^{2+} ions, however, probably stabilizes the transition state of the reaction favoring catalysis while the effect of H^+ is mainly manifested at the ground state. It would be interesting to see if the subtle interplay between Mg^{2+} and H^+ binding at the active site of *Mun*I is also important in the regulation of cleavage activity/binding specificity of other restriction enzymes.

ACKNOWLEDGMENT

We thank A. Lagunavicius for the help in protein purification, advice, and suggestions. We are also grateful to MBI "Fermentas" for the generous gift of enzymes used in this study.

REFERENCES

1. Stakenas, P. S., Zaretskaya, N. M., Maneliene, Z. P., Mauricas, M. M., Butkus, V. V., and Yanulaitis, A. A. (1992) *Mol. Biol. 26*, 546−557.
2. Pingoud, A., and Jeltsch, A. (1997) *Eur. J. Biochem. 246*, 1−22.
3. Siksnys, V., Zareckaja, N., Vaisvila, R., Timinskas, A., Stakenas, P., Butkus, V., and Janulaitis, A. (1994) *Gene 142*, 1−8.
4. Lagunavicius, A., and Siksnys, V. (1997) *Biochemistry 36*, 11086−11092.

5. Lagunavicius, A., Grazulis, S., Balciunaite, E., Vainius, D., and Siksnys, V. (1997) *Biochemistry 36*, 11093−11099.
6. Fersht, A. (1985) *Enzyme structure and mechanism*, W. H. Freeman and Company, New York.
7. Glusker, J. P. (1991) *Adv. Protein Chem. 42*, 1−76.
8. Groll, D. H., Jeltsch, A., Selent, U., and Pingoud, A. (1997) *Biochemistry 36*, 11389−401.
9. Gutfreund, H. (1995) in *Kinetics for the life sciences*, Cambridge University Press, Cambridge, UK.
10. Terry, G. J., Jack, W. E., and Modrich P. (1987) *Gene Amplif. Anal. 5*, 103−118.
11. Taylor, J. D., and Halford, S. E. (1989) *Biochemistry 28*, 6198−6207.
12. Yang, C. C., Baxter, B. K., and Topal, M. D. (1994) *Biochemistry 33*, 14918−14925.
13. Nobbs, T. J., Szcelkun, M. D., Wentzell, L. M., and Halford, S. E. (1998) *J. Mol. Biol. 281*, 419−432.
14. Hinsch, B., and Kula, M.-R. (1981) *Nucleic Acids Res. 9*, 3159−3174.
15. Jack, W. E., Terry, B. J., and Modrich, P. (1982) *Proc. Natl. Acad. Sci. U.S.A. 79*, 4010−4014.
16. Saenger, W. (1984) *Principles of Nucleic Acid Structure*, Springer-Verlag, New York.
17. Gordon-Beresford, R. M. H., Van Belle, D., Giraldo, J., and Wodak, S. (1996) *Proteins 25*, 180−194.
18. Kostrewa, D., and Winkler, F. K. (1995) *Biochemistry 34*, 683−696.
19. Johnson, K. A. (1995) *Methods Enzymol. 249*, 38−61.
20. Erskine S. G., Baldwin G. S., and Halford S. E. (1997) *Biochemistry 36*, 7567−7576.
21. Nardone, G., Wastney, M. E., and Hensley, P. (1990) *J. Biol. Chem. 265*, 15308−15315.
22. Zebala, J., Choi, J., and Barany, F. (1992) *J. Biol. Chem. 267*, 8097−8105.
23. Siksnys, V., and Pleckaityte, M. (1993) *Eur. J. Biochem. 217*, 411−419.
24. Halford, S. E., and Goodall, A. J. (1988) *Biochemistry 27*, 1771−1777.
25. Hensley, P., Nardone, G., and Chirikjian, J. G. (1990) *J. Biol. Chem. 265*, 15300−15307.
26. Lukat, G. S., Stock, A. M., and Stock, J. B. (1990) *Biochemistry 29*, 5436−42.
27. Oda, Y., Yamazaki, T., Nagayama, K., Kanaya, S., Kuroda, Y., and Nakamura, H. (1994) *Biochemistry 33*, 5275−84.

BI982456N